Available online at www.sciencedirect.com

SCIENCE DIRECT®

Journal of Molecular Catalysis A: Chemical 199 (2003) 49–56

JOURNAL OF MOLECULAR CATALYSIS A: CHEMICAL

www.elsevier.com/locate/molcata

An in situ STM study on Sb electrodeposition on Au(1 1 1): irreversible adsorption and reduction, underpotential deposition and mutual influences

Qiong Wu, Wang-Huo Shang, Jia-Wei Yan, Bing-Wei Mao*

State Key Laboratory for Physical Chemistry of Solid Surface, Department of Chemistry, Xiamen University, Xiamen 361005, China

Received 28 April 2002; received in revised form 1 July 2002; accepted 1 July 2002

Abstract

We present an in situ STM study on submonolayer Sb electrodeposition on Au(1 1 1). Different approaches have been employed to study Sb irreversible adsorption, the redox behavior of the Sb(III) adspecies with and without the influence of UPD and vice versa. The oxygenous Sb(III) is adsorb on Au(1 1 1) surface at potentials between 0.2 and 0.55 V, which is very likely in the form of in-plane oriented SbO^+ layer conjugated with the sulfate. In the solutions containing only sulfuric acid, this anion bound film undergoes a subtle structural change after the completion of discharge from Sb(III) to Sb(0) state at ∼0 V. In the Sb(III) containing solutions, the film type of structure of the adspecies is destroyed at the potential where Sb UPD takes place and more Sb can be incorporated, leading to structural transition to a worm-like network. Alloys at least involving two top layers of the surface are formed accompanying the structural transition. The Sb UPD without precedent with the irreversible adsorption proceeds by forming monoatomic high alloy islands of ∼10 nm in diameter. The apparent simple surface morphology provides evidence con that the channels within the complex worm-like network may well be a result of oxygen removal from the in-plane orientated SbO^+ layer and alloy formation as well.

Keywords: STM study; Sb electrodeposition; Au(1 1 1)

1. Introduction

It is well known that surface physical and chemical properties can be changed significantly by foreign metal adatoms/adspecies. Underpotential deposition (UPD) [1–3] and immersion method [4,5] are two effective electrochemical approaches for surface modification with submonolayer of metal adatoms/adspecies. Metal UPD concerns with electroreduction of metal ions from solution at electrode potentials that can be substantially less negative than that required for their bulk deposition. The immersion method, on the other hand, deals with the reduction as well as the oxidation of metal adspecies that has been introduced onto the electrode spontaneously at open circuit from solutions containing the metal ions. Metal adatoms/adspecies of varying coverage can be obtained by both approaches, which provides basis for, e.g. alteration of electrocatalytic activities [1,6–9] as well as introduction of surfactants crucial for a desired growing mechanism in metal thin film formation [10–12].

In recent years, studies on co-UPD [13] or sequential UPD [14] of more than one metal and adsorption of UPD adatoms and irreversibly adsorbed species [15]

* Corresponding author. Tel.: +86-592-2183051; fax: +86-592-2085349.
E-mail address: bwmao@xmu.edu.cn (B.-W. Mao).

1381-1169/03/$ – see front matter © 2003 Elsevier Science B.V. All rights reserved.
doi:10.1016/S1381-1169(03)00017-7

have also been reported. As a matter of fact, UPD may be precedent with the reduction of the irreversibly adsorbed species of its own [16,17]. Investigation under this circumstance would provide information that can help understand the dynamics of UPD and reduction of irreversibly adsorbed species (or adspecies) under the perturbation of each other. However, while extensive work has been carried out to elucidate the UPD adlayer structure utilizing the structural sensitive techniques such as scanning tunneling microscopy [18,3] and in situ X-ray diffraction [19], investigations of immersion prepared adspecies and their redox behavior are limited, in general, to conventional electrochemical methods. There is an increasing need to employ structural sensitive techniques to study metal submonolayer deposition including irreversible adsorption and redox behavior of the adspecies. Efforts in this aspect would be valuable for a full understanding of metal submonolayer deposition.

Sb is one of the typical elements that can be irreversibly adsorbed on metal surfaces such as Pt [4,5] and Au [16]. The Pt single crystal electrodes modified with the irreversibly adsorbed Sb have shown enhanced electrocatalytic activities towards electrooxidation of small organic molecules [20–22]. Sb is of interest also because, as a surfactant, it has been found in UHV to promote layer-by-layer growth mechanism in the metal thin film formation [11]. In this paper, we report an in situ STM study on Sb electrodeposition of submonolayer quantity on Au(1 1 1). With the strategies for studying the irreversible adsorption, the redox behavior with and without the influence of UPD and vice versa, our study aims to provide direct structural views to help gain deep insight into individual processes as well as their mutual interference.

2. Experimental

Au single crystal beads were prepared following the Calavilier method [23]. One of the (1 1 1) facets of the bead was used directly for in situ STM measurements. For conventional electrochemical measurements, the single crystal bead was oriented and polished to expose large enough (1 1 1) plane. Prior to each experiment, the working surface was subjected to electrochemical polishing and flame annealing in H_2 followed by cooling under N_2. The irreversible adsorption of Sb(III) on Au(1 1 1) was achieved via immersion method. The STM measurements and electrochemical measurements were performed either on a Sb(III) covered Au(1 1 1) surface in a supporting electrolyte of 0.5 M H_2SO_4 or on a Au(1 1 1) surface in contact with the sulfuric acid solution containing different amount of Sb(III) species. Detailed procedures for different approaches will be stated in Section 3. The in situ STM measurements were performed on Nanoscope IIIa with electrochemically etched and thermosetting polyethylene insulated W tips. A saturated calomel electrode (SCE) and a platinum wire were used as reference electrodes for electrochemical and in situ STM measurements, respectively. Potentials quoted in this work are, however, versus SCE. All solutions were prepared from AR chemicals with Millipore water.

3. Results and discussions

Solution chemistry suggests that the dominant form of Sb_2O_3 in acidic solution (pH = 0–1) is oxygenous Sb(III) (SbO^+) [24]. The amount and stability of the irreversibly adsorbed Sb(III) on Au(1 1 1) depend on its equilibrium with the Sb(III) species in the solution as well as the acidity of the solution. The cyclic voltammograms for reduction and oxidation of the adsorbed Sb(III) in solutions free of Sb(III) is shown as the inset of Fig. 1. It suggests a fractional coverage of 0.29 ML of Sb (either Sb(0) or Sb(III)), assuming a three-electron reduction from Sb(III) to Sb(0) and reported as a fraction of total number of Au(1 1 1) sites. Subsequent cycling causes partial removal of the adsorbed Sb(III).

In the Sb(III) containing solutions, with the bulk deposition at ~ -0.18 V, similar amount of adsorbed Sb(III) can be obtained on the surface. Cyclic voltammograms were recorded after stable *i–E* curves were obtained. Cycling into different cathodic potentials allows to distinguish the UPD of Sb (marked with D_2 at -0.05 V in Fig. 1) from the reduction of irreversibly adsorbed Sb(III) (D_1 at ~ 0 V). The anodic peaks A_2–A_4 are mixed features of UPD stripping associated with D_2 and oxidation of Sb(0) back to Sb(III) associated with D_1. The difference in the anodic features in comparison with that recorded in the solution free of Sb(III) implies that the irreversibly adsorbed Sb(III) has experienced a structural

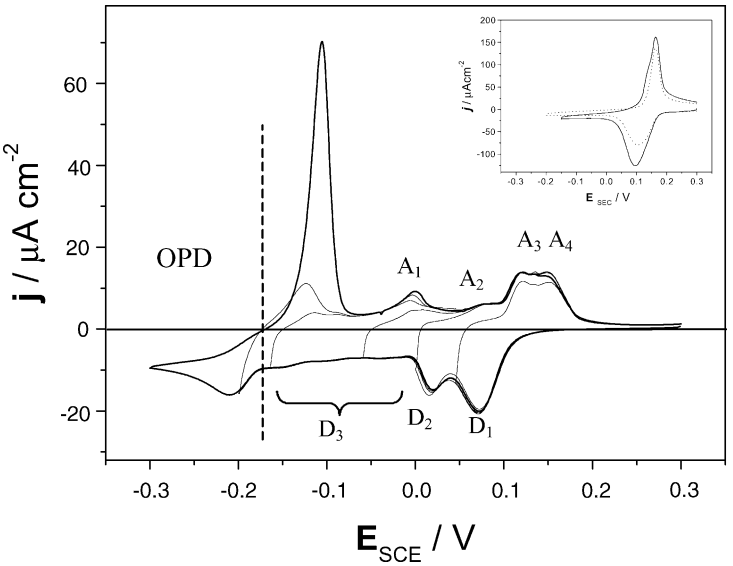

Fig. 1. Cyclic voltammograms of Au(1 1 1) in 0.5 M H_2SO_4 solution containing saturated (∼0.5 mM) Sb_2O_3 with sweep rate of 5 mV s^{-1}. Inset is the CVs of Au(1 1 1) electrodes covered with irreversibly adsorbed Sb(III) in 0.5 M H_2SO_4 free of Sb(III) with sweep rate of 50 mV s^{-1}. The solid and dashed lines indicate the first and second cycles, respectively.

transformation after the potential excursion into the UPD region. The charge flux associated with the UPD is rather small (∼0.15 ML). In addition, there is a steady cathodic residual current in a considerably wide potential range marked with D_3. It is believed that D_3 arises from further deposition of UPD Sb while A_1 corresponds to its dissolution. Most likely the process involves surface alloying at a kinetic limitation with a very slow rate. The general behavior on the cyclic voltammograms is consistent with that of previous electrochemical studies [16].

In situ STM experiments were performed with four different approaches in order to follow the irreversible adsorption of Sb(III), the reduction of the irreversibly adsorbed Sb(III), the UPD of Sb and the influence between the later two processes, respectively. In the first approach, irreversible adsorption of Sb(III) onto Au(1 1 1) was monitored under potential control at 0.3–0.4 V in the Sb(III) containing solution. Adsorption took place at 0.4 V but only with very small amount (Fig. 2a). The bright round disks are Au islands squeezed out during the lifting of the thermally induced reconstruction, while the light small spots are the Sb(III) adspecies at the initial stage of immersion. Slight negative potential shift to 0.36 V promotes considerably fast adsorption and an Sb(III) containing layer covered the entire surface in 18 min (Fig. 2b and c). As is shown in Fig. 2b, the Au step height is 0.25 nm and the adsorbed Sb(III) containing layer is of monoatomic height of ∼0.12 nm measured with respect to the uncovered region of the surface. This value is consistent with the ionic radius of 0.15 nm for Sb^{3+}. Taking into account the dominant form of SbO^+ for Sb(III) under the present experimental condition, the discrepancy between the apparent full coverage of the adsorbed Sb(III) layer and the small charge flux associated with the reduction of the Sb(III), which is equivalent of 0.29 ML, suggests an in-plane orientation of the adsorbed SbO^+. It is further inferred that a conjugate layer of sulfate stabilizes the in-plane oriented SbO^+ species. This conjugate sulfate seems to be transparent to STM imaging and does not contribute to the height of the adspecies layer. Small area images show that the Sb(III) layer is highly disordered (Fig. 2d) so that atomic resolution imaging was not achieved. We mention that the immersion potential (0.3–0.4 V) for Sb irreversible adsorption falls into the double layer region of a bare Au(1 1 1). Sulfate adsorption on the bare Au(1 1 1) in this potential region is weak [25,26]. However, this does not violate with the formation

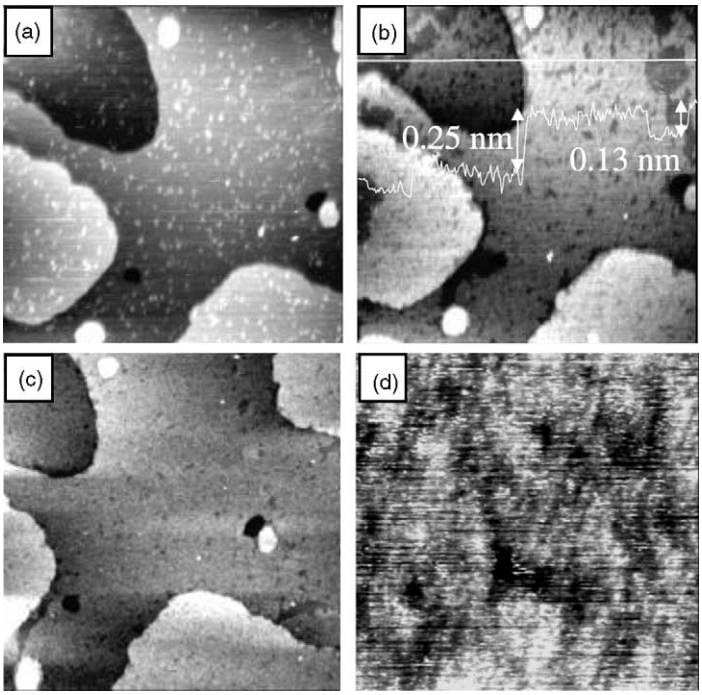

Fig. 2. Irreversible adsorption of oxygenous Sb(III) from 0.5 M H_2SO_4 solution saturated with Sb_2O_3 at 0.4 V (a), 0.36 V (b, c, d). An apparent full coverage of Sb(III) was reached after resting at 0.36 V for 18 min (c). The small area image of the adsorbed layer is given by (d). Scan size: 200 nm × 200 nm (a–c) and 20 nm × 20 nm (d).

of a conjugated sulfate layer since it is obvious that the highly and positively charged SbO^+ would induce adsorption of correspondingly large amount of sulfate.

In the second approach, the oxidation and reduction of the adsorbed Sb(III) was studied without the influence from solution species. To do so, the STM measurement was paused after a layer of Sb(III) adspecies was formed to allow for substitution of the solution in the STM cell with that free of Sb(III) by sucking and refilling for three to four times under potential control. The subsequent measurement was performed in the solution free of Sb(III) (Fig. 3). As can be seen, the original sharper and close-packed features of the morphology at 0.3 V (Fig. 3a) became relatively loosely packed at 0.03 V after the completion of the reduction process of Sb(III) (Fig. 3b). On reversing the potential, this morphology maintained until the potential was set back to 0.3 V (Fig. 3c). After resting at this potential for about 20 min, the film was able to restore close to its original morphology with sharp features of the Sb(III) adspecies but with significantly decreased coverage (Fig. 3d). The surface became smooth in the region where Sb(III) had been removed. No pits were observed, excluding the alloy formation during the redox processes.

It has been reported that anion can have strong influence on the stability as well as the redox behavior of the irreversibly adsorbed species [27]. The film morphological change during the reduction and oxidation of the Sb(III) adspecies is subtle in the present work and this indicates that it may involve only processes such as substitution of conjugate species while the adspecies remains unchanged in terms of relative positions within the film. It is conceivable that upon discharge of Sb(III) into Sb(0), the conjugate sulfate anions decrease their affinity with Sb(0) and very likely give way to less strongly binding water molecules, making the film with a relatively loose structure. The decrease in coverage after reduction/oxidation cycles is believed to be a consequence of escape of the Sb(III) adspecies during

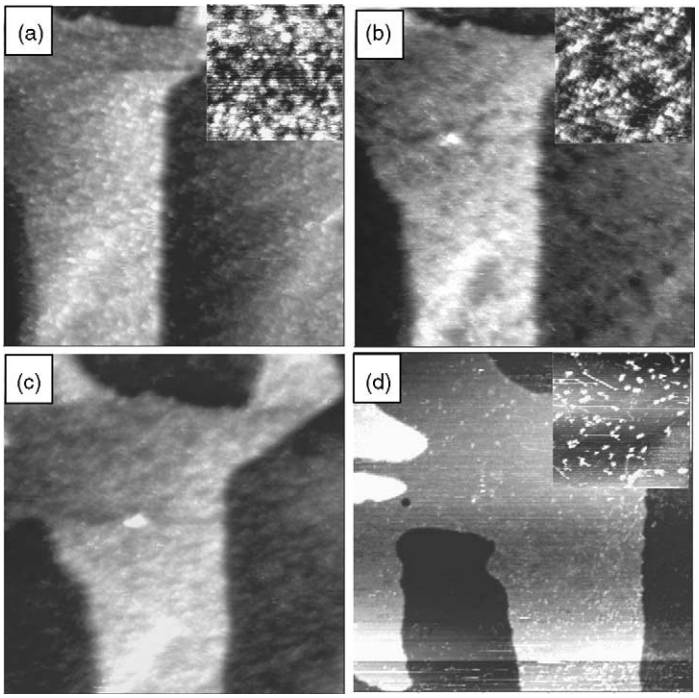

Fig. 3. Sequence of STM images showing morphological changes during reduction and oxidation of Sb(III) adspecies on Au(1 1 1) in 0.5 M H_2SO_4 solution. Sb adsorption onto Au(1 1 1) was achieved by immersing in sulfuric acid solution saturated with Sb_2O_3 at 0.3 V for 10 min. The immersion solution was replaced with pure sulfuric acid solutions under potential control. (a) Film of oxygenous Sb(III) adspecies with small aggregates at 0.3 V; (b) film of loosely packed network after reduction of the adspecies at the potential region of 0.03 to −0.03 V; (c) Reversal of potential back to 0.3 V and (d) 20 min after (c) with partial removal of the adspecies. Scan size: 130 nm × 130 nm. Inset: 16.3 nm × 16.3 nm (a), 34.5 nm × 34.5 nm (b) and 32 nm × 32 nm (c).

substitution of the conjugate species from sulfate to water molecules and vice versa.

In the third approach, Sb UPD was studied without precedent by the irreversible adsorption. The experiments were conducted by introducing an Sb(III) containing solution at the potential where only UPD could be initiated. The final concentration of Sb(III) was 10 times diluted than the saturation concentration. Sb was electrochemically deposited as soon as Sb(III) species diffuses to the surface. Thus, the irreversible adsorption could be avoided before UPD. Large amount of monoatomic high islands were formed immediately at −0.07 V accompanied by slight reshaping of the step edge (Fig. 4b). The average height of the islands is 0.28 nm, in agreement with the monoatomic height of Sb or Au. The islands became bigger when further deposition was promoted at decreasing potentials (Fig. 4c). Some of the islands coalesce to form deposit domains. Atomic resolution images were not achieved for these island surfaces. On anodic sweeping of potential to strip the UPD Sb at 0.4 V, islands were left over on the surface and pits were formed on the terraces as well as those left over islands (Fig. 4d) indicating surface alloying upon Sb UPD.

As the final approach, STM measurements were performed directly after the formation of a layer of irreversibly adsorbed Sb(III) in the solution containing Sb(III) species to study the reduction of Sb(III) adspecies with the influence of Sb UPD. Fig. 5 shows a sequence of potential-dependent surface following Fig. 2c. It can be seen that the film-like morphology sustained up to −0.09 V (Fig. 5a), where subtle changes of the film structure may have been involved as has just been discussed. A significant structural transition occurred at −0.04 V where the UPD (corresponding to D_2 in Fig. 1) is completed (Fig. 5b and c). The newly evolved surface morphology is substantially different from either the film structure

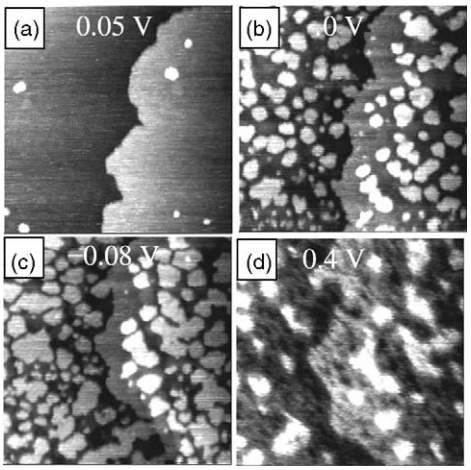

Fig. 4. STM images of Au(1 1 1) in the supporting electrolyte of 0.5 M H_2SO_4 at 0.05 V (a), after introduction of Sb(III) containing solution (with final concentration of 0.1 mM) at 0 V (b) and −0.08 V (c), and after stripping of UPD accompanied by irreversible adsorption at 0.4 V (d). Scan size: 200 nm × 200 nm.

of reduced Sb(III) adspecies in the second approach (Fig. 3b) or the island morphology of pure UPD of Sb in the third approach (Fig. 4b and c). A remarkable shrinking of the adsorbed layer and rotten of the top most layers of the Au surface that are in direct contact with the adsorbed layer were observed, breaking up integrity of the film as well as the top most Au surface. This is discerned by the partial exposure of the surface that was originally covered by the upper layers of Au and Sb(III) (see regions indicated by arrows in Fig. 5a and b). In addition, a light but eye-catching three-dimensional aggregation has been involved during the process. In a few minutes, a clear two-dimensional worm-like network structure evolved with small amount of bright dots scattered especially at the junctions of the network indicated by circles (Fig. 5c). The height of the connections of the network (or the depth of the channels) is 0.22 ± 0.1 nm with respect to the lower terrace, and widths of the connections as well as the channels are ∼5 nm on average.

Based on the cyclic voltammetric measurements, the completion of UPD at −0.04 V contributes extra 0.15 ML to the Sb coverage. Obviously, the worm-like structure is a result of a UPD-driven structural transition involving oxygen removal that destroys the film structure and release considerable amount of surface sites. The increase in Sb coverage upon UPD also promoted surface alloying. This is further supported

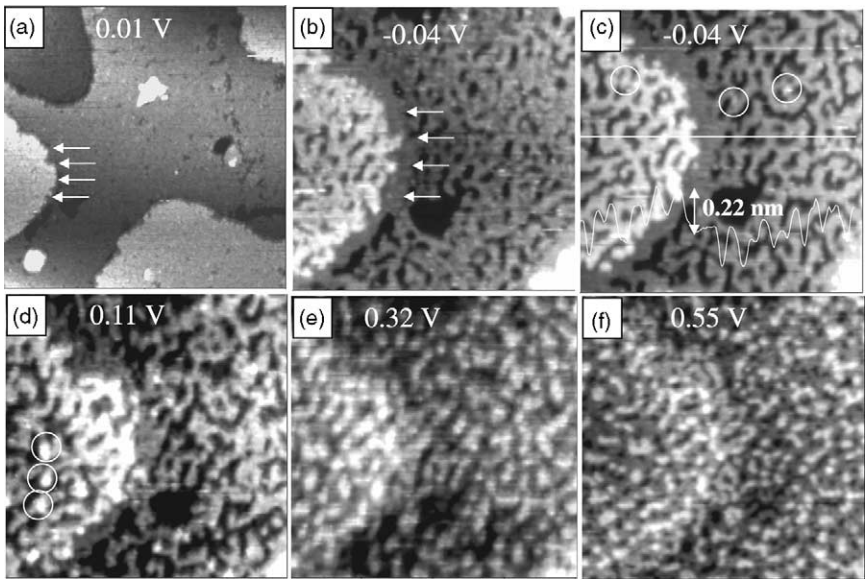

Fig. 5. STM images showing potential-dependent morphological change of Au(1 1 1) in 0.5 M H_2SO_4 solution containing saturated Sb_2O_3. (a) Following Fig. 2c and after reduction of the Sb(III) adspecies at 0.01 V; (b) during and (c) after the completion of Sb UPD in 3 min; (d) after stripping of UPD Sb; (e) oxidation and/or re-adsorption of Sb(III) adspecies; (f) desorption of Sb(III) adspecies. Scan size: 200 nm × 200 nm.

by the pits and protrusions generated after stripping of the UPD Sb by anodic sweeping up to the completion of A_2 at 0.11 V (Fig. 5d). It is believed that the alloyed Sb is only partially stripped at this stage, and the remaining surface is still heavily intermixed so that its structure is in sharp contrast with the film-like morphologies of Sb(III) adspecies either in reduced or oxidized state shown by Fig. 3a and b, respectively. Complete dealloying became possible at higher potential of 0.32 V, followed by the irreversible adsorption of Sb(III) on a further fragmentized surface (due to dealloying), making it apparently three-dimensional protrusion (Fig. 5e). Complete desorption of the Sb(III) adspecies at potentials positive of +0.55 V restore the surface with two-dimensional features, though severely fragmentized. This allows identification of the pits both in the first and second layers. It clearly indicates that alloy had developed beyond the first layer of the surface directly underneath the Sb. It is known that $AuSb_2$ is the only form of bulk alloy between Au and Sb [28]. Obviously, the surface alloy composition is much different from that of the bulk because otherwise the submonolayer coverage of Sb would not even alloy with half of the Au layer directly underneath. The surface alloy in the present work likely involves two layers of surface Au atoms though identification of the alloy composition is not possible on the basis of the present data.

4. Summary

With four different approaches, we have monitored Au(1 1 1) surfaces with Sb irreversible adsorption, the reduction and oxidation of the Sb(III) adspecies with and without the influence of solution species of Sb(III), and the Sb UPD without precedent with the irreversible adsorption, respectively. The irreversible adsorption of the oxygenous Sb(III) (SbO^+) onto Au(1 1 1) surface occurs at potentials between 0.2 and 0.55 V in the form of in-planed oriented configuration conjugated with sulfate above the Sb(III) adlayer. The directional bond of SbO^+ is randomly oriented on the surface preventing atomic resolution observation of detailed arrangement of SbO^+. In the absence of UPD, the reduction and oxidation of Sb(III) adspecies corresponds to subtle changes of the film morphology. In the Sb(III) containing solution where several processes can take place subsequently, the film type of structure of the Sb adspecies is destroyed at the potential where Sb UPD takes place and more Sb can be incorporated, leading to the structural transition to a worm-like structure. The channels within the complex worm-like network may well be a result of oxygen removal from the in-plane orientated SbO^+ layer. Alloy formation has been involved upon UPD regardless of the irreversible adsorption. The results have demonstrated a close interplay between the irreversible adsorption of Sb(III) and UPD of Sb. It is expected that such a study would provide a better understanding of both processes.

Acknowledgements

The financial support from Natural Science Foundation of China (NSFC No. 29973040, 29833060 and 20021002) is gratefully acknowledged.

References

[1] R.R. Adzic, in: H. Gerischer (Ed.), Advance in Electrochemistry and Electrochemical Engineering, vol. 13, Wiley/Interscience, New York, 1984, p. 159.
[2] D.M. Kolb, in: H. Gerischer, Ch.W. Tobias (Eds.), Advances in Electrochemistry and Electrochemical Engineering, vol. 11, Wiley, New York, 1978, p. 125.
[3] E. Herrero, L.J. Buller, H.D. Abrunã, Chem. Rev. 101 (2001) 1897, and reference therein.
[4] M.M.P. Jansen, J. Moolhuysen, Electrochim. Acta 21 (1976) 861.
[5] M.M.P. Jansen, J. Moolhuysen, Electrochim. Acta 21 (1976) 869.
[6] R. Parsons, T. VanderNoot, J. Electroanal. Chem. 257 (1988) 9.
[7] N. Gaeler, K. Jacobi, W. Ranke, Surf. Sci. 75 (1978) 355.
[8] G. Kokkinidis, J.M. Leger, C. Lamy, J. Electroanal. Chem. 242 (1988) 221.
[9] D. Shmeisser, K. Jacobi, Surf. Sci. 88 (1979) 138.
[10] J. Camarero, J. Ferrón, V. Cros, L. Gomez, A.L. Vázquez de Parga, J.M. Gallego, J.E. Prieto, J.J. de Miguel, R. Miranda, Phys. Rev. Lett. 81 (1998) 850.
[11] H.A. van der Vegt, J. Vrijmoeth, R.J. Behm, E. Vlieg, Phys. Rev. B 57 (1998) 4127.
[12] J. Camarero, T. Graf, J.J. de Miguel, R. Miranda, W. Kuch, M. Zharnikov, A. Dittschar, C.M. Scheider, J. Krishcner, Phys. Rev. Lett. 76 (1996) 4428.

[13] C. Schroter, T. Solomun, Ber. Bunsen-Ges. Phys. Chem. 100 (1996) 1257.
[14] S. Takami, G.K. Jennings, P.E. Laibints, Langmuir 17 (2001) 441.
[15] S.P.E. Smith, H.D. Abrunã, J. Phys. Chem. B 103 (1999) 6764.
[16] G. Jung, C.K. Rhee, J. Electroanal. Chem. 436 (1997) 277.
[17] G.J.H. Park, C.K. Rhee, J. Electroanal. Chem. 436 (1998) 243.
[18] A.A. Gewirth, B.K. Niece, Chem. Rev. 97 (1997) 1129.
[19] B.M. Ocko, J. Wang, in: C.A. Melendres, A. Tadjeddine (Eds.), Synchrotron Techniques in Interfacial Electrochemistry, Kluwer, Dordrecht, 1994, p. 127.
[20] J.M. Feiliu, A. Fernandez-Vega, A. Alada, J. Electroanal. Chem. 256 (1988) 149.
[21] Y.Y. Yang, S.G. Sun, Y.J. Gu, Z.Y. Zhou, C.H. Zhen, Electrochim. Acta 46 (2001) 4339.
[22] A. Fernandez-Vega, J.M. Liu, A. Aldaz, J. Electroanal. Chem. 258 (1989) 101.
[23] J. Clavilier, D. Armand, S.G. Sun, M. Petit, J. Electroanal. Chem. 205 (1987) 267.
[24] F.A. Cotton, Advanced Inorganic Chemistry, Wiley, New York, 1972.
[25] G.J. Edens, X.P. Gao, M.J. Weaver, J. Electroanal. Chem. 375 (1994) 357.
[26] K. Ataka, M. Osawa, Langmuir 14 (1998) 951.
[27] S.P.E. Smith, H.D. Abrunã, J. Phys. Chem. B 102 (1998) 3506.
[28] V. Simić, Z. Marinkoviæ, J. Mater. Sci. 33 (1998) 561.